

Enhancement of the upper critical field in codoped iron-arsenic high-temperature superconductors

F. Weickert,^{1,2} M. Nicklas,¹ W. Schnelle,¹ J. Wosnitza,³ A. Leithe-Jasper,¹ and H. Rosner¹

¹⁾ *Max-Planck-Institut für Chemische Physik fester Stoffe, 01187 Dresden, Germany*

²⁾ *Los Alamos National Laboratory, Los Alamos, New Mexico 87545, USA*

³⁾ *Hochfeld-Magnetlabor Dresden, Helmholtz-Zentrum Dresden-Rossendorf, 01328 Dresden, Germany*

(Dated: 9 March 2021)

We present the first study of codoped iron-arsenide superconductors of the 122 family $(\text{Sr}/\text{Ba})_{1-x}\text{K}_x\text{Fe}_{2-y}\text{Co}_y\text{As}_2$ with the purpose to increase the upper critical field H_{c2} compared to single doped $\text{Sr}/\text{BaFe}_2\text{As}_2$ materials. H_{c2} was investigated by measuring the magnetoresistance in high pulsed magnetic fields up to 64 T. We find, that H_{c2} extrapolated to $T = 0$ is indeed enhanced significantly to ≈ 90 T for polycrystalline samples of $\text{Ba}_{0.55}\text{K}_{0.45}\text{Fe}_{1.95}\text{Co}_{0.05}\text{As}_2$ compared to ≈ 75 T for $\text{Ba}_{0.55}\text{K}_{0.45}\text{Fe}_2\text{As}_2$ and $\text{BaFe}_{1.8}\text{Co}_{0.2}\text{As}_2$ single crystals. Codoping thus is a promising way for the systematic optimization of iron-arsenic based superconductors for magnetic-field and high-current applications.

PACS numbers: 74.25.Dw; 74.25.Fy; 74.25.Op; 74.62.Dh

I. INTRODUCTION

The recent discovery of Fe based superconductors¹ has attracted great interest in the solid-state-physics community. Up to date, several classes of superconducting Fe based materials have been found, such as the $RE\text{OFeAs}$ (1111, $RE = \text{rare-earth element}$), $(\text{Li},\text{Na})\text{FeAs}$ (111),² $A\text{Fe}_2\text{As}_2$ (122, $A = \text{Ca, Sr, Ba}$),³ and FeSe (11)⁴ systems. Superconductivity (SC) at critical temperatures T_c up to 55 K appears when the materials are doped appropriately or are pressurized. Beside the rather high T_c , these superconductors have a very high upper critical field H_{c2} . In addition, the small anisotropy of the 11 and 122 compounds in comparison with 1111-type and especially cuprate-based high- T_c superconductors, rises reasonable hope, that they will be available in some years for high magnetic-field and high-current applications. Another important factor for a prospective technical implementation are mechanical and processing properties. In particular, the 122 systems, including the non-superconducting parent compounds, are metals or semimetals with good mechanical properties for manufacturing.

Concerning the microscopic mechanism, in the compounds of the 1111, 122, and 111 families, the Fe-As layers are considered to be the structural elements carrying the SC. A charge doping of these layers is most easily accomplished – as inspired by the cuprate superconductors – by an appropriate charge transfer from the interspacing layer. The tuning of the charge within the Ba layer by K in $\text{Ba}_{1-x}\text{K}_x\text{Fe}_2\text{As}_2$ (*indirect* hole doping) does not change the volume of the unit cell significantly, but the ratio c/a of the lattice parameters increases. It was found, that the substitution of Ba by K in the crystal structure of BaFe_2As_2 leads to a rapid suppression of the spin density wave (SDW) ordering and to the emergence of SC.³ The optimum value of $T_c = 38$ K is observed for a K substitution of 40%.³ Indirect electron doping failed until recently, when it was discovered that the substitu-

tion of Ca in CaFe_2As_2 by La leads to a stabilization of the structurally collapsed phase and to superconducting signals at temperatures up to 45 K.⁵ Concerning upper critical fields, H_{c2} was found to be only weakly dependent on the direction of the field for K doped BaFe_2As_2 .⁶ $\text{Ba}_{0.55}\text{K}_{0.45}\text{Fe}_2\text{As}_2$, which is closest to optimal doping with a high T_c of 32.2 K, has a maximal value of 68 T at $T = 14$ K ($H \perp c$)⁷ and the extrapolation to zero Kelvin gives an H_{c2}^0 of 75 T.

The *direct* doping of the Fe-As layers by substituting transition elements on the Fe site^{8,9} or by replacing arsenic by phosphorous¹⁰ was discovered to be also an option to induce SC in 1111 and 122 compounds. Doping of Co or Ni on the Fe site, which is equivalent to electron doping, leads to the suppression of the SDW order and the development of SC as well. In 122 compounds, small cobalt concentrations of $y = 0.125 - 0.2$ are sufficient to reach the highest transition temperature of 18–23 K for the SC.^{8,9,11} Also isoelectronic substitution of Fe by, e.g., Ru was successful to generate SC,¹² however, the required concentration is much higher than for electron doping. Hole doping, e.g., with Mn, has not been successful in neither suppressing the SDW ordering nor inducing SC.¹³

The T_c of directly doped 122-type iron-arsenic superconductors is about a factor of two lower than for those obtained by indirect doping. This may be understood from the larger disorder in the Fe-As planes in the former compounds.⁸ For $\text{BaFe}_{2-y}\text{Co}_y\text{As}_2$ the upper critical field for samples close to optimal doping ($y = 0.2$) was estimated experimentally to be 45 T at 10 K,¹⁴ but the steep initial slope of $H_{c2}(T)$ in the temperature-magnetic-field phase diagram suggests an H_{c2}^0 in the same order of magnitude like for K doped BaFe_2As_2 . Subsequent studies on $\text{BaFe}_{0.84}\text{Co}_{0.16}\text{As}_2$ single crystals with same T_c of 22 K confirm these findings and reveal a critical field H_{c2}^0 of 55 T in the limit $T \rightarrow 0$ K.¹⁵ Thus, in spite of the lower T_c , in-plane doping seems to be beneficial for obtaining

high values of $dH_{c2}(T)/dT|_{T=T_c}$.

Similar effects are observed for SrFe₂As₂ doped with K or Co, respectively. Here, the optimal K content is between 0.2 and 0.4 with a corresponding maximum T_c of 38 K,^{16,17} however, for an optimally doped sample a detailed magnetic-field study was not carried out so far. In the case of Co doping, the concentration with the highest T_c of 19.2 K was estimated to be 0.2 in a study on polycrystalline samples.⁸ Results of the temperature dependence of the upper critical field on epitaxial films of the same Co concentration with $T_c=17.1$ K reveal a maximum H_{c2} of approximately 47 T.¹⁸

In magnetic fields, SC is suppressed mainly by two effects, (i) Pauli limiting, where the Cooper pairs gain more energy than the superconducting condensation energy ΔE_{SC} via the Zeemann effect and, (ii) by orbital limiting, where the kinetic energy of the electron pairs exceeds ΔE_{SC} . Latter effect can be suppressed by introducing disorder to the system, which systematically enhances the scattering rate. This leads to an increase of H_{c2} and is in particular effective in superconductors with large mean-free-path such as MgB₂.¹⁹ In contrast, Fe based superconductors have a rather small mean-free-path due to a small Fermi velocity and a significant increase of the upper critical field by disorder is unlikely. However, electron and hole doping modifies the shape of the multiple Fermi sheets and can lead to a rise of the upper critical field as well.¹⁹

In the present study, we investigate BaFe₂As₂ and SrFe₂As₂ materials, which were doped simultaneously on the Ba and on the Fe site. Conceptually, our method of codoping is based on the superior transition temperatures obtained in superconductors of the 122 materials by indirect doping, combined with an increase of the slope $dH_{c2}(T)/dT|_{T=T_c}$ at T_c due to a manipulation of the electronic band structure of the Fe-As layers by direct doping. The results of our feasibility study strongly suggest, that by codoping it is possible to push the upper critical field to higher values. We want to emphasize that no optimization of the concentration levels has been done so far, but our investigations on Ba_{0.55}K_{0.45}Fe_{1.95}Co_{0.05}As₂ and Sr_{0.6}K_{0.4}Fe_{1.95}Co_{0.05}As₂ establish a straightforward route for an improvement of the superconducting upper critical field in iron-arsenide superconductors for high-field and high-current applications.

Until recently,⁵ no electron doping of the Fe-As layers in 122 systems via charge transfer could be achieved and up to now no hole doping within the Fe-As layers was successful in generating SC. We therefore decided to try a *counter* doping by K (holes) in the interspacing layers and by Co (electrons) within the Fe-As layers. In order to achieve an optimum T_c , this implies that some overdoping has to be made with one kind of dopant in order to compensate for the counter doping. Since T_c might be expected to be low with large levels of Co doping, we decided to overdope only slightly above the optimal concentration with K ($0.4e^+ + 0.05e^+$ for Ba 122, $\approx 0.35e^+ + 0.05e^+$ for Sr 122), and to compensate with the same

amount of electrons ($-0.05e^-$) with Co.

II. EXPERIMENTAL TECHNIQUES

The samples were synthesized by standard powder metallurgical techniques as described elsewhere^{8,13} in an argon-gas glove-box system. First, stoichiometric blends of reacted starting materials with nominal compositions Fe₂As, Co₂As, SrAs, BaAs, and KAs were pressed in stainless steel dies into cylindrical pellets without any additional lubricants. Then, these pellets were welded into tantalum containers and sealed under vacuum in quartz ampoules. Heat treatment at 850 °C for 10 days with up to 4 intermediate regrinding and compaction steps completed the sample preparation. Afterwards, the samples were cut by a wire-saw and characterized by metallography, also performed under argon atmosphere, and wave-length dispersive (WDXS) microprobe analysis. Successful substitution of alkaline-earth with potassium and iron by cobalt could be corroborated by quantitative chemical analysis of all investigated samples. We found, that the exact composition values Ba_{0.53(6)}K_{0.47(2)}Fe_{1.94(6)}Co_{0.05(1)}As_{1.99(6)} and Sr_{0.6(1)}K_{0.4(1)}Fe_{1.95(5)}Co_{0.06(1)}As_{1.96(6)} deviate only negligible from the nominal concentrations Ba_{0.55}K_{0.45}Fe_{1.95}Co_{0.05}As₂ and Sr_{0.6}K_{0.4}Fe_{1.95}Co_{0.05}As₂. The tetragonal lattice parameters were established to $a = 3.9063(2)$ Å, $c = 13.365(1)$ Å and $a = 3.8918(2)$ Å, $c = 12.9095(8)$ Å for the Ba and Sr compound, respectively. Small amounts of Fe₂As as an impurity phase, which grains are randomly dispersed within the matrix, could also be detected. The material shows a fair stability towards air and humidity, but starts to degrade after several weeks.

Resistivity and specific heat were measured between 1.8 K and 300 K in a commercial system (PPMS, Quantum Design). The heat capacity was determined with a thermal-relaxation technique and resistance with a conventional 4-probe method. Magnetic-susceptibility data were taken around the superconducting phase transition in a SQUID magnetometer (MPMS, Quantum Design). The measurement of the magnetoresistance in fields up to 64 T took place at the Dresden High Magnetic Field Laboratory (HLD) in a liquid-nitrogen cooled pulsed-magnet equipped with a ⁴He flow cryostat. The pulsed magnets at HLD are energized via a 24 kV capacitor bank. We use a standard 4-probe AC technique with currents of about 2 mA and a measuring frequency of 15 kHz. The current was applied parallel to the magnetic-field direction in order to avoid parasitic Hall-contributions in the results. We observe a small difference in the magnetoresistance between up and down sweep of the magnet pulse indicating eddy-current heating, albeit the cross section of the sample was chosen to be as small as possible ($< 0.2 \times 0.3$ mm², see insets in Figs. 4 and 5). An estimate of the induced heat in the samples revealed an increase in temperature of about $\Delta T = 0.5$ K at 25 K in

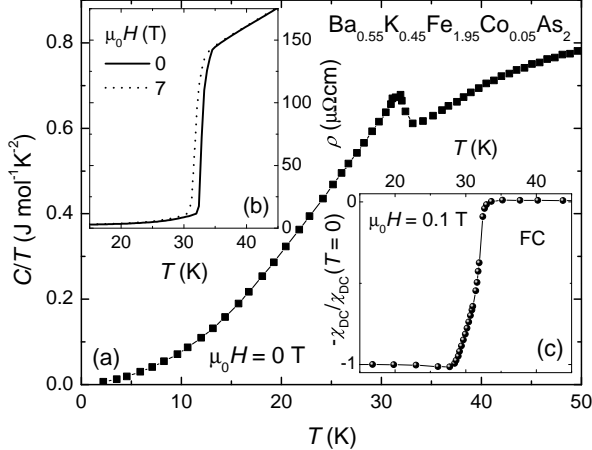


FIG. 1. Temperature dependence of (a) the specific heat in zero magnetic field, plotted as C/T vs. T , (b) the resistivity $\rho(T)$ in $\mu_0 H = 0$ and 7 T, and (c) the magnetic susceptibility $\chi_{DC}(T)$, measured at 0.1 T in field-cooled mode and normalized by the low-temperature value of the $\text{Ba}_{0.55}\text{K}_{0.45}\text{Fe}_{1.95}\text{Co}_{0.05}\text{As}_2$ polycrystalline sample.

the normal conducting state. Nevertheless, we only use data taken during the up sweep of the magnet pulse to ensure that the indicated temperatures are correct.

III. RESULTS AND DISCUSSION

We performed a comprehensive characterization of the samples in order to ensure the good quality of our quinary compounds. Metallography on polished surfaces of the sample combined with WDXS analysis confirm the composition and good homogeneity.

The susceptibility data, taken in a field of 0.1 T, of $\text{Ba}_{0.55}\text{K}_{0.45}\text{Fe}_{1.95}\text{Co}_{0.05}\text{As}_2$ are shown in Fig. 1(c). A sharp drop at T_c to large negative values is observed during cooling the sample in field (FC). The observed onset of the transition is at $T_{c,\text{on}} = 32.5$ K.

Figure 1(a) shows the total specific heat of the same sample. Specific heat is an excellent tool to judge on the quality of a superconducting compound since it is a bulk probe. The size of the step-like specific-heat anomaly at T_c directly measures the condensation entropy of the superconductor. Moreover, the width of the step in the present case is predominately determined by the chemical inhomogeneities within the material. We observe a large and sharp anomaly at T_c . The data between 24 K and 42 K were fitted with a lattice term plus a superconducting contribution for a quantitative analysis. We model the lattice background by a smooth polynomial equation, because no suitable non-superconducting reference sample is available. The electronic term can be modeled either with the Bardeen-Cooper-Schrieffer (BCS) theory in the weak-coupling limit, where the specific-heat

jump at T_c obeys $\Delta c_{el} = 1.43\gamma_n T_c$, or by the classical two-fluid model. Latter is a rather good description for the thermodynamics of a SC with moderately strong electron-phonon coupling and yields $2\gamma_n T_c$ for Δc_{el} . For $\text{Ba}_{0.55}\text{K}_{0.45}\text{Fe}_{1.95}\text{Co}_{0.05}\text{As}_2$, the two-fluid model fits better (40% lower least-squares deviation) our specific-heat data, than the BCS function. The resulting T_c is 32.5 K, obtained from the midpoint of the transition, and the value for the reduced specific-heat jump $\Delta c_{el}/T_c$ can be estimated to $116 \text{ mJ mol}^{-1} \text{ K}^{-2}$. Both, the assumption of moderately strong coupling as well as the estimated value for $\Delta c_{el}/T_c$ are in agreement with recent findings in Ref. [20] for $\text{Ba}_{0.68}\text{K}_{0.32}\text{Fe}_2\text{As}_2$, which has a T_c of 38.5 K. Therefore, we conclude, that the major sacrifice for codoping with 2.5% cobalt is the lowering of T_c by 6 K compared to optimal K single doping while the condensation entropy is only slightly affected. Another quality criterion from specific-heat data is the size of the residual normal electronic coefficient γ_{res} in zero field. Most probably such a contribution indicates normal conducting parts within the sample, however, the presence of non-gapped parts of the Fermi surface in certain compositions of Fe-As superconductors cannot be excluded.⁸ We find a particular low γ_{res} of $2.4 \text{ mJ mol}^{-1} \text{ K}^{-2}$ in our polycrystalline sample. For comparison, single-crystalline samples of $\text{Ba}_{0.6}\text{K}_{0.4}\text{Fe}_2\text{As}_2$ showed $\gamma_{\text{res}} = 1.2 \text{ mJ mol}^{-1} \text{ K}^{-2}$, while for $\text{BaFe}_{2-x}\text{Co}_x\text{As}_2$ crystals $\gamma_{\text{res}} = 3.7 \text{ mJ mol}^{-1} \text{ K}^{-2}$ was reported.^{20,21} The initial Debye temperature of $\text{Ba}_{0.55}\text{K}_{0.45}\text{Fe}_{1.95}\text{Co}_{0.05}\text{As}_2$ is $232.(3) \text{ K}$.

The electrical resistivity decreases continuously between room temperature and 32.5 K (data not shown), which is characteristic for metallic behavior. The value slightly above T_c [Fig. 1(b)] of about $135 \mu\Omega \text{ cm}$ indicates low impurity concentrations in the sample. Figure 1(b) already gives an idea about the enormous tolerance of the superconducting state in $\text{Ba}_{0.55}\text{K}_{0.45}\text{Fe}_{1.95}\text{Co}_{0.05}\text{As}_2$ against magnetic fields. In a field of 7 T, the critical temperature is suppressed by only 1.5 K.

Our second sample, $\text{Sr}_{0.6}\text{K}_{0.4}\text{Fe}_{1.95}\text{Co}_{0.05}\text{As}_2$ (data not shown), displays in the resistivity and magnetic susceptibility a behavior similar to $\text{Ba}_{0.55}\text{K}_{0.45}\text{Fe}_{1.95}\text{Co}_{0.05}\text{As}_2$, but at lower T_c of 29 K. The anomaly in the specific heat at the superconducting phase transition is less pronounced in this material, which is no indication for bad sample quality, but typical for Sr 122 iron-arsenides.⁸ Those compounds have a lower electronic Sommerfeld coefficient, γ , indicating a lower electronic density of states at the Fermi level and, therefore, generally lower condensation entropy. However, the transition in $\text{Sr}_{0.6}\text{K}_{0.4}\text{Fe}_{1.95}\text{Co}_{0.05}\text{As}_2$ is also considerably broader than for Ba based material, suggesting some degree of chemical inhomogeneity in the sample. This observation is supported by the more than 2 times higher resistivity value of $325 \mu\Omega \text{ cm}$ just above T_c in the normal conducting state.

The high-field magnetoresistance as a function of applied magnetic field is plotted in Fig. 2 for $\text{Ba}_{0.55}\text{K}_{0.45}\text{Fe}_{1.95}\text{Co}_{0.05}\text{As}_2$ and in Fig. 3 for

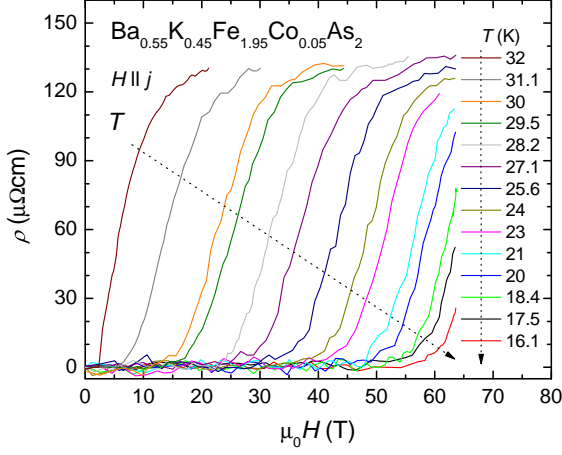


FIG. 2. (color online) Longitudinal magnetoresistance $\rho(H)$ ($H \parallel j$) measured up to 64 T in pulsed magnetic fields for temperatures between 16.1 K and 32 K of a $\text{Ba}_{0.55}\text{K}_{0.45}\text{Fe}_{1.95}\text{Co}_{0.05}\text{As}_2$ polycrystal.

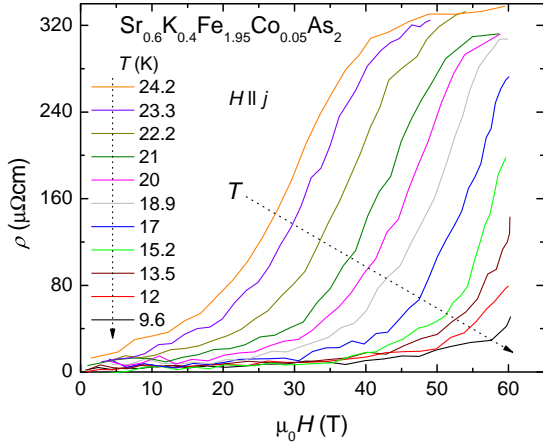


FIG. 3. (color online) Longitudinal magnetoresistance $\rho(H)$ ($H \parallel j$) measured up to 60 T in pulsed magnetic fields for temperatures between 9.6 K and 24.2 K of a $\text{Sr}_{0.6}\text{K}_{0.4}\text{Fe}_{1.95}\text{Co}_{0.05}\text{As}_2$ polycrystal.

$\text{Sr}_{0.6}\text{K}_{0.4}\text{Fe}_{1.95}\text{Co}_{0.05}\text{As}_2$. The superconducting transition in the first material is rather sharp and the width does almost not change with decreasing temperature. In contrast, in $\text{Sr}_{0.6}\text{K}_{0.4}\text{Fe}_{1.95}\text{Co}_{0.05}\text{As}_2$ the transition width is about 30 T for 23.3 K just below T_c .

The broadening of the superconducting transition for polycrystalline samples is associated with the anisotropy of the upper critical field between different crystallographic directions.²² In tetragonal systems, such as the 122 compounds presented here, the ratio $\gamma_H = H_{c2}^{\perp c} / H_{c2}^{\parallel c}$ with $H_{c2}^{\perp c} > H_{c2}^{\parallel c}$ has to be considered. The magne-

toresistance is dominated by the higher critical field due to a random orientation of crystal grains in the sample. As long as they are superconducting, the micro crystals oriented along the direction of the higher critical field ($H \perp c$) short-circuit the electrical current in the sample. Thus, the onset of SC in the $\rho(H)$ curves is a good approximation for $H_{c2} \perp c$. The appearance of finite resistivity, on the other hand, can be used to identify the lower limit of the distribution of critical fields, namely $H_{c2} \parallel c$. Nevertheless, one has to keep in mind, that the anisotropy γ_H obtained from magnetoresistance measurements is usually underestimated.²²

The experimental results in Fig. 2 reveal, that the critical field in $\text{Ba}_{0.55}\text{K}_{0.45}\text{Fe}_{1.95}\text{Co}_{0.05}\text{As}_2$ is quite isotropic with values of γ_H around 3.5 near T_c , which decrease below 1.5 at lower temperatures. These ratios are comparable to those observed for individually K or Co doped single crystals $\text{Ba}_{0.55}\text{K}_{0.45}\text{Fe}_2\text{As}_2$ ⁷ and $\text{BaFe}_{1.8}\text{Co}_{0.2}\text{As}_2$ ¹⁴ and emphasize the essentially three-dimensional character of SC in the investigated material. For $\text{Sr}_{0.6}\text{K}_{0.4}\text{Fe}_{1.95}\text{Co}_{0.05}\text{As}_2$ the anisotropy is significant higher and can be estimated to 4.5 at 23.2 K with decreasing tendency down to 3 at lower temperatures. The values are higher than those observed for $\text{SrFe}_{1.8}\text{Co}_{0.2}\text{As}_2$ film samples (< 1.6),¹⁸ but they are consistent with recent observations on single crystals of $\text{Sr}_{1-x}\text{Na}_x\text{Fe}_2\text{As}_2$,²³ where γ_H varies between 8 and 2.

The magnetic field – temperature ($H - T$) phase diagram of the superconducting phase transition is obtained from resistivity data as a function of temperature in small static magnetic fields and from the magnetoresistance experiments at constant temperature in pulsed fields. Before H_{c2} can be estimated from the magnetoresistance, the data need to be scaled due to a non-negligible temperature and field dependence of the resistivity in the normal conducting state, $\rho(T, H)$ for $H > H_{c2}(T)$. Both effects have been considered to be quadratic in temperature $\Delta\rho(T) \sim T^2$ and field $\Delta\rho(H) \sim H^2$, respectively.

We estimate the onset of SC (90% ρ), the midpoint of the superconducting transition (50% ρ), and the onset of dissipation in the sample (10% ρ). The data are displayed in Fig. 4 for $\text{Ba}_{0.55}\text{K}_{0.45}\text{Fe}_{1.95}\text{Co}_{0.05}\text{As}_2$ and in Fig. 5 for $\text{Sr}_{0.6}\text{K}_{0.4}\text{Fe}_{1.95}\text{Co}_{0.05}\text{As}_2$. We observe in $\text{Ba}_{0.55}\text{K}_{0.45}\text{Fe}_{1.95}\text{Co}_{0.05}\text{As}_2$ a smooth crossover from data obtained in static fields to those from pulsed-field experiments. In the case of $\text{Sr}_{0.6}\text{K}_{0.4}\text{Fe}_{1.95}\text{Co}_{0.05}\text{As}_2$, pulse-field data are missing between 25 and 28 K, because we focused on the high-field region in the phase diagram during our granted magnet time at the pulse-field facility. Open symbols in the phase diagrams represent extrapolated values $H_{c2}^{90\%}$ and $H_{c2}^{50\%}$ for temperatures, where up to 64 T ($\text{Ba}_{0.55}\text{K}_{0.45}\text{Fe}_{1.95}\text{Co}_{0.05}\text{As}_2$) and up to 60 T ($\text{Sr}_{0.6}\text{K}_{0.4}\text{Fe}_{1.95}\text{Co}_{0.05}\text{As}_2$) only 10% of ρ was achieved, assuming a continuous smooth increase of the magnetoresistance at H_{c2} of similar shape as for curves at higher temperatures.

One important parameter characterizing the superconducting state, which is directly linked to the orbital crit-

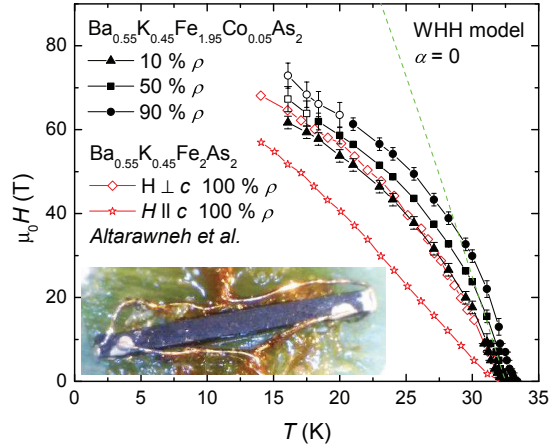


FIG. 4. (color online) Temperature – magnetic-field phase diagram of the superconducting transition in $\text{Ba}_{0.55}\text{K}_{0.45}\text{Fe}_{1.95}\text{Co}_{0.05}\text{As}_2$ estimated by magnetoresistance measurements. The (black) symbols label H_{c2} for the 10% (triangles), 50% (squares), and 90% (dots) criterion of the resistivity. Closed symbols are experimental data, whereas data marked with open symbols are extrapolated values. Theoretical expectations of the WWH model without Pauli limiting (Maki parameter $\alpha = 0$) are indicated by the (green) dashed line. The (red) open stars and diamonds are data of Altarawneh *et al.*⁷ on a single crystal $\text{Ba}_{0.55}\text{K}_{0.45}\text{Fe}_2\text{As}_2$ for magnetic field $H \parallel c$ and $H \perp c$, respectively. The photo inset shows the 4.5 mm long polycrystalline sample mounted for the pulsed-field experiment.

ical field, is the initial slope $dH_{c2}/dT|_{T=T_c}$. A fitting of our 50% ρ data reveals a steep slope of -10.1 T K^{-1} at T_c for $\text{Ba}_{0.55}\text{K}_{0.45}\text{Fe}_{1.95}\text{Co}_{0.05}\text{As}_2$, which is rather high among all 122 iron-arsenic based superconductors, but was also found in $\text{Ba}_{0.68}\text{K}_{0.32}\text{Fe}_2\text{As}_2$.²⁴ The initial slope for $\text{Sr}_{0.6}\text{K}_{0.4}\text{Fe}_{1.95}\text{Co}_{0.05}\text{As}_2$ instead is with -5.5 T K^{-1} a typical value for this class of materials.^{22,25}

The Werthammer-Helfand-Hohenberg (WHH) model^{26,27} is commonly used to evaluate the $T = 0$ limit of the upper critical field, H_{c2}^0 . Accounting only for orbital effects where the Maki parameter α is 0, the break-down of SC is predicted for

$$H_{c2,\text{orb}}^0 = 0.69T_c \left| \frac{dH_{c2}}{dT} \right|_{T_c} \quad (1)$$

and it depends only on the initial slope and the transition temperature T_c . We show in both phase diagrams (Figs. 4 and 5) the expected WWH curves as dashed lines. The calculated maximal values $H_{c2,\text{orb}}^0$ for $\text{Ba}_{0.55}\text{K}_{0.45}\text{Fe}_{1.95}\text{Co}_{0.05}\text{As}_2$ and $\text{Sr}_{0.6}\text{K}_{0.4}\text{Fe}_{1.95}\text{Co}_{0.05}\text{As}_2$ are 227 T and 110 T, respectively. The actual upper critical fields are much smaller than the predictions of the WWH model indicating the importance of Pauli spin-paramagnetism as pair-breaking mechanism for both compounds. This is in particular valid for the codoped

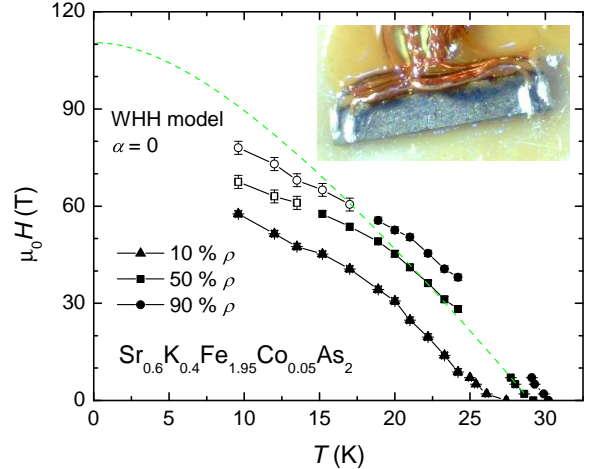


FIG. 5. (color online) Temperature – magnetic-field phase diagram of the superconducting transition in $\text{Sr}_{0.6}\text{K}_{0.4}\text{Fe}_{1.95}\text{Co}_{0.05}\text{As}_2$. The symbols label H_{c2} for the 10% (triangles), 50% (squares), and 90% (dots) criterion of the resistivity ρ . Closed symbols are experimental data, whereas data marked with open symbols are extrapolated values. Theoretical predictions of the WWH model without Pauli limiting (Maki parameter $\alpha = 0$) are indicated by the (green) dashed line. The photo inset shows the 3.5 mm long polycrystalline sample mounted for magnetoresistance measurements in pulsed fields.

Ba sample.

We compare in Fig. 4 our results on $\text{Ba}_{0.55}\text{K}_{0.45}\text{Fe}_{1.95}\text{Co}_{0.05}\text{As}_2$ with data taken on $\text{Ba}_{0.55}\text{K}_{0.45}\text{Fe}_2\text{As}_2$ single crystals⁷ obtained by radio-frequency (RF) penetration-depth experiments. The comparison shows very clearly that, despite of similar superconducting transition temperatures of about 32.5 K, the critical field of the codoped sample is significant larger than H_{c2} of $\text{Ba}_{0.55}\text{K}_{0.45}\text{Fe}_2\text{As}_2$ in the entire temperature range. We conclude, that extra cobalt doping in a small amount does not reduce the transition temperature, but increases the upper critical field significantly. Note, that we are comparing our upper-critical-field data using the 90% ρ criterion with H_{c2} values from the RF penetration-depth technique, which are basically equivalent to H_{c2} data obtained from the 100% ρ rule. This implies, that the difference between the $H_{c2}(T)$ curves of both materials will increase further when using the same experimental technique.

Finally, the upper critical field in the zero-temperature limit is extrapolated. Following the curvature of $H_{c2}(T)$ we expect 90 T for $\text{Ba}_{0.55}\text{K}_{0.45}\text{Fe}_{1.95}\text{Co}_{0.05}\text{As}_2$, which is an increase by more than 15% compared to single doped $\text{Ba}_{0.55}\text{K}_{0.45}\text{Fe}_2\text{As}_2$.⁷ For $\text{Sr}_{0.6}\text{K}_{0.4}\text{Fe}_{1.95}\text{Co}_{0.05}\text{As}_2$ no high field $H_{c2}(T)$ data on $\text{Sr}_{0.6}\text{K}_{0.4}\text{Fe}_2\text{As}_2$, the reference compound exist. However, a comparison with results on $\text{SrFe}_{1.8}\text{Co}_{0.2}\text{As}_2$ ¹⁸ suggests a similar enhance-

ment considering the different T_c 's.

IV. SUMMARY AND OUTLOOK

To summarize, we have measured the magnetoresistance of polycrystalline samples of $\text{Ba}_{0.55}\text{K}_{0.45}\text{Fe}_{1.95}\text{Co}_{0.05}\text{As}_2$ and $\text{Sr}_{0.6}\text{K}_{0.4}\text{Fe}_{1.95}\text{Co}_{0.05}\text{As}_2$ between the superconducting transition temperature and about 10 K in pulsed high magnetic fields up to 64 T in order to estimate the upper critical field of the superconducting phase transition. We found that, (i) the codoped sample $\text{Ba}_{0.55}\text{K}_{0.45}\text{Fe}_{1.95}\text{Co}_{0.05}\text{As}_2$ shows in the entire phase diagram significant larger critical fields than the optimally doped $\text{Ba}_{0.55}\text{K}_{0.45}\text{Fe}_2\text{As}_2$ compound and, (ii) that the critical field in the 0 K limit is enhanced by more than 15%, despite of the same transition temperature of about 32.5 K. The results for the Sr containing 122 material are similar to those of the Ba compound, whereas H_{c2}^0 is 80% higher than for only cobalt doped samples. However, the critical temperatures and the homogeneity of the Sr samples is lower compared to the Ba system. This is reflected in a significant broader superconducting phase transition.

Our study establishes *codoping* as the route to follow for enhancing the upper critical field on the iron-arsenide superconductors with only a minor effect on the transition temperature. In order to obtain even higher upper critical fields at $T = 0$, a detailed optimization of the K content with respect to the Co concentration for the highest possible T_c and critical fields is required. We are convinced that our findings are an important step forward in the development of iron-arsenide materials for the usage in high magnetic-field and high-current applications.

FW and MN acknowledge financial funding by the MPG Research Initiative: *Materials Science and Condensed Matter Research at the Hochfeldmagnetlabor Dresden*. Part of this work was supported by EuroMagNET II under the EC contract 228043. MN, JW, ALJ, and HR thank the Deutsche Forschungsgemeinschaft (DFG) for financial support through SPP 1458.

REFERENCES

- ¹Y. Kamihara, T. Watanabe, M. Hirano, and H. Hosono, *J. Am. Chem. Soc.* **130**, 3296 (2008).
- ²J. H. Tapp, Z. Tang, B. Lv, K. Sasmal, B. Lorenz, P. C. W. Chu, and A. M. Guloy, *Phys. Rev. B* **78**, 060505(R) (2008).
- ³M. Rotter, M. Tegel, and D. Johrendt, *Phys. Rev. Lett.* **101**, 107006 (2008).
- ⁴F.-C. Hsu, J.-Y. Luo, K.-W. Yeh, T.-K. Chen, T.-W. Huang, P. M. Wu, Y.-C. Lee, Y.-L. Huang, Y.-Y. Chu, D.-C. Yan, and M.-K. Wu, *Proc. Nat. Acad. Sci. USA* **105**, 14 262 (2008).

- ⁵*See, e.g.*, B. Lv, L. Z. Deng, M. Gooch, F. Y. Wei, Y. Y. Sun, J. Meen, Y. Y. Xue, B. Lorenz, C. W. Chu, arXiv:1106.2157.
- ⁶H. Q. Yuan, J. Singleton, F. F. Balakirev, S. A. Baily, G. F. Chen, J. L. Luo, N. L. Wang, *Nature* **457**, 565 (2009).
- ⁷M. M. Altarawneh, K. Collar, C. H. Mielke, N. Ni, S. L. Bud'kov, and P. C. Canfield, *Phys. Rev. B* **78**, 220505(R) (2008).
- ⁸A. Leithe-Jasper, W. Schnelle, C. Geibel, and H. Rosner, *Phys. Rev. Lett.* **101**, 207004 (2008).
- ⁹A. S. Sefat, R. Jin, M. A. McGuire, B. C. Sales, D. J. Singh, and D. Mandrus, *Phys. Rev. Lett.* **101**, 117004 (2008).
- ¹⁰S. Jiang, H. Xing, G. Xuan, C. Wang, Z. Ren, C. Feng, J. Dai, Z. Xu, and G. Cao, *J. Phys.: Condens. Matter* **21**, 382203 (2009).
- ¹¹N. Ni, M. E. Tillmann, J.-Q. Yan, A. Kracher, S. T. Hannahs, S. L. Bud'ko, and P. C. Canfield, *Phys. Rev. B* **78**, 214515 (2008).
- ¹²W. Schnelle, A. Leithe-Jasper, R. Gumeniuk, U. Burkhardt, D. Kasinathan, and H. Rosner, *Phys. Rev. B* **79**, 214516 (2009).
- ¹³D. Kasinathan, A. Ormeci, K. Koch, U. Burkhardt, W. Schnelle, A. Leithe-Jasper, and H. Rosner, *New J. Phys.* **11**, 025023 (2009).
- ¹⁴A. Yamamoto, J. Jaroszynski, C. Tarantini, L. Balicas, J. Jiang, A. Gurevich, D. C. Larbalestier, R. Jin, A. S. Sefat, M. A. McGuire, B. C. Sales, D. K. Christen, and D. Mandrus, *Appl. Phys. Lett. B* **94**, 062511 (2009).
- ¹⁵M. Kano, Y. Kohama, D. Graf, F. Balakirev, A. S. Sefat, M. A. McGuire, B. C. Sales, D. Mandrus, S. W. Tozer, *J. Phys. Soc. Jap.* **78**, 0847191 (2009).
- ¹⁶G.-F. Chen, Z. Li, G. Li, W.-Z. Hu, J. Dong, J. Zhou, X.-D. Zhang, P. Zheng, N.-L. Wang, and J.-L. Luo, *Chin. Phys. Lett.* **25**, 3403 (2008).
- ¹⁷G. F. Chen, Z. Li, J. Dong, G. Li, W. Z. Hu, X. D. Zhang, X. H. Song, P. Zheng, N. L. Wang, and J. L. Luo, *Phys. Rev. B* **78**, 224512 (2008).
- ¹⁸S. A. Baily, Y. Kohama, H. Hiramatsu, B. Maiorov, F. F. Balakirev, M. Hirano, and H. Hosono, *Phys. Rev. Lett.* **102**, 117004 (2009).
- ¹⁹C. Tarantini, A. Gurevich, *Bulletin MRS* **36**, 626 (2011) *and references therein*.
- ²⁰P. Popovich, A. V. Boris, O. V. Dolgov, A. A. Golubov, D. L. Sun, C. T. Lin, R. K. Kremer, and B. Keimer, *Phys. Rev. Lett.* **105**, 027003 (2010).
- ²¹K. Gofryk, A. S. Sefat, M. A. McGuire, B. C. Sales, D. Mandrus, J. D. Thompson, E. D. Bauer, and F. Ronning, *Phys. Rev. B* **81**, 184518 (2010).
- ²²G. Fuchs, S.-L. Drechsler, N. Kozlova, G. Behr, A. Köhler, J. Werner, K. Nenkov, R. Klingeler, J. Hamann-Borrero, C. Hess, A. Kondrat, M. Grobosch, A. Narduzzo, M. Kupfer, J. Freudenberger, B. Büchner, and L. Schultz, *Phys. Rev. Lett.* **101**, 237003 (2008).
- ²³L. Jiao, J. L. Zhang, F. F. Balakirev, G. F. Chen, J. L. Luo, N. L. Wang, and H. Q. Yuan, *J. Phys. Chem.*

- Solids **72**, 423 (2011).
- ²⁴V. A. Gasparov, F. Wolff-Fabris, D. L. Sun, C. T. Lin, and J. Wosnitzer, *JETP Letters* **93**, 26 (2011).
- ²⁵M. Putti, I. Pallecchi, E. Bellingeri, M. R. Cimberle, M. Tropeano, C. Ferdeghini, A. Palenzona, C. Tarantini, A. Yamamoto, J. Jiang, J. Jaroszynski, F. Kametani, D. Abraimov, A. Polyanskii, J. D. Weiss, E. E. Hellstrom, A. Gurevich, D. C. Larbalestier, R. Jin, B. C. Sales, A. S. Sefat, M. A. McGuire, D. Mandrus, P. Cheng, Y. Jia, H. H. Wen, S. Lee, and C. B. Eom, *Supercond. Sci. Technol.* **23**, 034003 (2010) *and references therein*.
- ²⁶E. Helfand and N. R. Werthamer, *Phys. Rev.* **147**, 288 (1966).
- ²⁷N. R. Werthamer, E. Helfand, and P. C. Hohenberg, *Phys. Rev.* **147**, 295 (1966).